Journal of the Nigerian Association of Mathematical Physics,

Volume 8 (*November 2004*).

The modelling of instabilities in liquid-liquid miscible displacement processes by the Galerkin-based finite element method

K. I. Idigbe,
Department of Petroleum Engineering,
University of Benin, Benin City, Edo State, Nigeria.

Abstract

The Galerkin-based finite element method has been used to successfully simulate the propagation of instabilities in the liquid-liquid miscible displacement process. The convective-dispersion equation is sufficient to model the liquid-liquid miscible displacement process under unstable conditions. The investigations reveal:

i. An unconditional instability which will not disappear with time,
ii. The rate of growth of the instabilities, tended to increased proportionally to a number to the M power, where M is the mobility ratio,
iii. The propagation of instabilities can be achieved through the actions of viscous, gravity and heterogeneous forces, and
iv. ***Heterogeneity in permeability introduces a macroscopic dispersion effect that attempts to stabilize the instabilities****.*

pp 173 - 176

1.0 Introduction

The liquid-liquid miscible displacement process is primarily governed by the convective-dispersion equations (1.1) and (1.2), which are non-linear.

$$-div\,\underset{\sim}{U}_{mix} \equiv -\nabla.\underset{\sim}{U}_{mix} = 0 \qquad (1.1)$$

$$\nabla\phi\,\underset{\sim}{D}\nabla c - \nabla.\left(c\,\underset{\sim}{U}_{mix}\right) = \phi\left(\partial c \big/ \partial t\right) \qquad (1.2)$$

Equation (1.2) describes the dimensionless volume concentration profile of the displacing miscible liquid, the solvent, at any point at any time. The first term of this equation represents the mixing phenomenon between the two fluids-solvent and oil, while the second term arises from the mass transport by convection. The term on the right accounts for the unsteady-state accumulation.

The effective dispersion term, $\underset{\sim}{D}$, is velocity dependent, while the mass average velocity, U_{mix}, depends on the solvent concentration through the mixture density and viscosity. Thus, equations (1.1) and (1.2) form a set of coupled, non-linear partial differential equations, sometimes referred to as phase and component balance equations [1].

The non-linearity of the set of partial differential equations precludes their analytical or exact closed-form solutions and hence, the necessity of approximate solutions.

In reservoir simulation studies, the finite difference and the finite element methods are the basic numerical techniques used to solve the non-linear partial differential equations [2, 3, 4, 5, 6]. In the present work, the finite

element method was used to solve the non-linear partial differential equations that govern the miscible displacement process.

Studies were initiated to investigate the following:

(i) The appropriateness of the set of non-linear partial differential equations to properly characterize the liquid-liquid miscible displacement process, and

(ii) The modeling of instabilities in the liquid-liquid miscible displacement process by the Galerkin based finite element method.

2.0 Formulation

To solve equations (1.1) and (1.2), we seek displacement in an *x, y, z* coordinate system, with flow in the positive x-direction. The miscible fluid enters the system at the face, $x = 0$, and leaves at the other face, $x = L$. The side boundaries are impermeable to flow defined by the conditions (flux-type) as:

$$-\partial\Phi/\partial y\,[0,z] = 0; \quad 0 \le z \le w \tag{2.1}$$

$$-\partial\Phi/\partial y\,[d,z] = 0; \quad 0 \le z \le w \tag{2.2}$$

$$-\partial\Phi/\partial z\,[y,0] = 0; \quad 0 \le y \le d \tag{2.3}$$

$$-\partial\Phi/\partial z\,[y,w] = 0; \quad 0 \le z \le d \tag{.2.4}$$

$$-\frac{\partial c}{\partial y}[0,z] = 0; \quad 0 \le z \le w \tag{2.5}$$

$$-\frac{\partial c}{\partial y}[d,z] = 0; \quad 0 \le z \le w \tag{2.6}$$

$$-\frac{\partial c}{\partial z}[y,0] = 0; \quad 0 \le y \le d \tag{2.7}$$

$$-\frac{\partial c}{\partial y}[y,w] = 0; \quad 0 \le y \le d \tag{2.8}$$

Equivalently, equations (2.1) to (2.6) can be redefined in terms of the phase pressure, P. Φ is the flow potential

We can represent the system by a plane as shown in Figure 1. At the inlet boundary, the miscible fluid, the solvent, is introduced at a constant rate. At this boundary, the conditions that satisfy equations (1.1) and (1.2) are:

$$\frac{-K_x}{\mu}\left[\frac{\partial P}{\partial x} - \rho g \sin\theta\right] n_x + q_s = 0 \tag{2.9}$$

where q_s = a prescribed solvent flux, n_x = the direction cosine of the outward normal.

$$c\,[x, y, t] = c_o;\ t > 0,\ 0 \le y \le d \tag{2.10}$$
$$= 1$$

for pure solvent injection. At the outlet boundary, $x = L$, the conditions are:

$$P[x, y, t] = 0;\ t > 0,\ 0 \le y \le d \tag{2.11}$$
$$c[x, y, t] = 0;\ t > 0,\ 0 \le y \le d \tag{2.12}$$

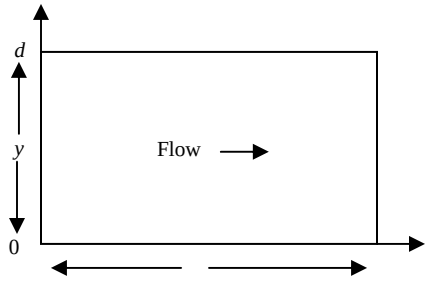

0 x L

Figure 1: A Model Plane of System

Let v and q be any admissible trial and test functions [7, 8, 9]. Since approximate solutions are sought to equations (1.1) and (1.2), a residual or error is defined for each equation as:

$$r_1 = F_1 [v_1 = P^*] \tag{2.13}$$

$$r_2 = F_2 [v_2 = c^*] \tag{2.14}$$

where F_1 and F_2 are differential operators, and P^* and c^* represent the approximate solutions to equations (1.1) and (1.2). The objective is the minimization of the errors involved in satisfying equations (1.1) and (1.2) by the approximate solutions, in a global manner. If the trial functions were the exact solutions, the residuals, r_1 and r_2, will vanish. We define weighted residual conditions for the equations as:

$$\int_A r_1 q_1 dA = 0 \tag{2.15}$$

$$\int_A r_2 q_2 dA = 0 \tag{2.16}$$

for sufficiently smooth test or weight functions, q_1 and q_2, and the integration are taken over the area A of the continuum.

Introducing the expressions for U_{mix} in the respective x and y dimensions into equation (2.15), we obtain a second-order partial differential equation in pressure:

$$\int_A q_1 \ (x_* + y_*) d\ A = 0 \tag{2.17}$$

where

$$x^* = \frac{\partial}{\partial x}\left[-0.00633\ \frac{K_x}{\mu}\left(\frac{\partial P_*}{\partial x} - \frac{\rho g \sin\theta}{144 g_c}\right)\right] \tag{2.18}$$

$$y^* = \frac{\partial}{\partial x}\left[-0.00633\ \frac{K_y}{\mu}\ \frac{\partial P_*}{\partial y}\right] \tag{2.19}$$

Equation (2.17) reveals a lack of symmetry in the formulation – the same order of derivatives of the trial and test functions does not exist. We desire a symmetric formulation – the same order of trial and test functions. For example, this is achieved as follows:

$$\int_A q_q\ \ y_*\ dA = \int \frac{\partial}{\partial y}\left[-.00633\ \frac{K_y}{\mu}\ \frac{\partial P_*}{\partial y} q_1\right] dA \quad + \int_A \left(-0.00633\ \frac{K_y}{\mu}\ \frac{\partial P_*}{\partial y}\ \frac{\partial q_1}{\partial y}\right) dA \tag{2.20}$$

Applying the Green-Gauss theorem to the first integral on the right side of equation (2.20) yields

$$\int_A \frac{\partial}{\partial y}\left[-0.00633\ \frac{K_y}{\mu}\ \frac{\partial P_*}{\partial y} q_1\right] dA = \int_{S_2}\left(-0.00633\ \frac{K_y}{\mu}\ \frac{\partial P_*}{\partial y} n_y\right) q_1 dS \tag{2.21}$$

When the expression on the right side of equation (2.21) is substituted for its equivalent term in equation (2.20), a symmetric formulation of the problem is obtained. Also, the expression on the right side of equation (2.21) defines the condition at the boundaries, $y = 0$ and $y = d$. These boundaries are impermeable, thus, equation (2.21) will vanish at these boundaries. The flux-type boundary condition is a natural consequence of the symmetric weighted residual formulation of the problem. Similarly for the x-contribution:

$$\int_{S_1}\left[-0.00633\ \frac{K_x}{\mu}\left(\frac{\partial P_*}{\partial x} - \frac{\rho g \sin\theta}{144 g_c}\right) n_x\right] q_1 dS + \int_A 0.00633 \frac{K_x}{\mu}\frac{\partial P_*}{\partial x}\frac{\partial q_1}{\partial x} dA = \int_A 0.00633 \frac{K_x}{\mu}\frac{\rho g \sin\theta}{144 g_c}\frac{\partial q_1}{\partial x} dA \tag{2.22}$$

The first term on the left side of equation (2.22) defines the condition at the boundaries, $x = 0$ and $x = L$. The second term on the right side of equation (2.20) and that on the left side of equation (2.22), give the contributions to the stiffness matrix.

In deriving the above equations, the trial and test functions are assumed to be admissible functions. They belong to a class of admissible functions for the problem [1]. This class has two properties. First, it is a linear space of functions, and second, it is infinite dimensional.
However, instead of tackling the infinite-dimensional problem, approximate solutions in a finite-dimensional space, are sought in the following form:

$$v_1 = P* \equiv P_N = \sum_{i=1}^{N} P_i(t)\phi(x,y) \tag{2.23}$$

$$v_2 = c* \equiv C_N = \sum_{i=1}^{N} c_i(t)\phi(x,y) \tag{2.24}$$

where the functions, ϕ (x, y) are called basis functions. The Galerkin weighted residual method is defined when the test functions are chosen identical to the basis functions.

While the Galerkin method provides an elegant strategy for constructing the approximate solutions to equations (1.1) and (1.2), it does not provide a systematic way of constructing reasonable basis functions, $\phi(x, y)$.

This difficulty is overcome by using the finite element method, which permits a general and systematic technique for constructing the basis functions for the Galerkin method.

3.0 Computational Aspects

The choice of the basis or shape functions and their degree is made after the discretization of the solution domain into finite elements. In the present study, C^0 quadrilateral finite elements were used for the discretization process. The 9-node Lagrangian finite elements were used in the simulation studies.

Settari et al. in [4] encountered difficulties with the 8-node serendipity elements in their solution of miscible problems. The 9-node Lagrangian finite elements have not been seriously tested in reservoir simulation studies, hence the decision to use them in the present work. All the simulation studies were performed with the 9-node bi-quadratic Lagrangian elements [1].

For the discretization of time, a fully implicit scheme was used to avoid any non-physical oscillations. A Fortran IV source program was written to do all computations. The source program consists of a main program and 16 subprograms.

4.0 Result

To model the propagation of any instability that may result in a liquid-liquid miscible displacement process, numerical simulation is required.

Figures (2) to (4) show the results of the numerical simulation studies that were performed using the Galerkin-based 9-node bi-quadratic Lagrangian finite elements. All instabilities were initiated at the inlet face, $x = 0$ by the condition of equation (2.10).

5.0 Discussions

From the results of the investigation, it is apparent that equations (1.1) and (1.2) are sufficient to model the liquid-liquid miscible displacement process under unstable conditions. Reference [1] through inspectional analysis, showed that some of the factors that characterize instabilities are implicitly imbedded in the equations.

Figure 2 shows an unconditional instability, which will not disappear with time. Perrine [11] reported that the only instability observed is conditional instability – one that will disappear after a sufficiently long time. Our investigations agree with the experimental findings of Habermann [12]. The value of N_s (N_S = 590.63 [1,10] greater than $4\pi^2$, demonstrates that the displacement will be unconditionally unstable.

When compared to Figure 3, Figure 2 shows that the rate of the growth of any instability tends to increase proportionally to a number of the M power, where M is the mobility ratio. At the injection of 0.5 PV, the instabilities had reached the outer boundary $x = L$, for $M = 20$.

Warren et al. in [13] and Perrine et al. in [14] noted that the effect of macroscopic dispersion in miscible displacement processes is to dampen the displacement fronts. Figures 4 shows the results of the simulation of initiated instabilities in a system with randomly placed permeabilities. By 0.5*PV*, the front had still not reached the outer boundary. The induced macroscopic dispersion by the presence of heterogeneity in permeability tended to dampen the instabilities. However, the instabilities were still propagated, but not as severe as that shown in Figures 2 and 3 for a homogeneous system.

6.0 Conclusions

The Galerkin-based 9-node bi-quadratic Lagrangian finite elements were used to successfully simulate the propagation of instabilities in liquid-liquid miscible displacement processes.

The investigations reveal;

i. An unconditional instability which will not disappear with time,

ii. The rate of growth of the instabilities, tended to increase proportionally to a number to the *M* power, where M is the mobility ration

iii. The propagation of instabilities can be achieved through the actions of viscous, gravity and heterogeneous forces,

iv. Heterogeneity in permeability introduces a macroscopic dispersion effect that attempts to stabilize the instabilities, and

Also the investigations show that the convective-dispersion equation is suitable to model unstable liquid-liquid miscible displacement processes.

References

[1] Idigbe, K.I. (1984): Application of Stability Theory and Finite Element Simulation to Characterize Miscible Displacements, Ph.D. Thesis submitted to the Department of Petroleum Engineering, Uni. of Texas at Austin, Austin, Texas, USA.

[2] Peaceman, D.W. and Rachford, H.H. (1962): Numerical Calculation of Multidimensional Miscible Displacement, Soc. Pet. Eng. Journal, pp. 327.

[3] Chaudhari, N.M. (1971): An Improved Numerical Technique for Solving Multidimensional Miscible Displacement Equation, Soc. Pet. Eng. Journal, pp 277-284.

[4] Settari, A., Price, H.S. and Duport, T. (1977): Development and Application of Variational Methods for Simulation of Miscible Displacement in Porous Media, Soc. Pet. Eng. Journal, pp 228-246.

[5] McMichael, C.L. and Thomas, Simulation by Galerkin Methods, Soc. Pet. Eng. Journal, pp 125-138.

[6] Yoon, Y.S. and Yeh, W.G. (1976): Parameter Identification in an Inhomogeneous Medium with the Finite Element Method, Soc. Pet. Eng. Journal, pp 217-226.

[7] Becker, E.B., Carey, G.F. and Oden, J.T. (1981): Finite Elements-An Introduction, Vol. 1, Prentice-Hall, Englewood Cliffs, New Jersey.

[8] Hinton, E. and Owen, D.R. J. (1979): An Introduction to Finite Element Computations, Pineridge Press Ltd., Swansea, U.K.

[9] Segarlind, L.J. (1976): Applied Finite Element Analysis, John Wiley & Sons, Inc., New York.

[10] Idigbe, K. I. (2003): An Appropriate Dimensionless Number for the Scaling and Modeling of Miscible Displacement Processes, Journal of Engineering for Development, Faculty of Engineering, Univ. of Benin, pp. 1-8.

[11] Perrine, R.L. (1961): The Development of Stability Theory for Miscible Liquid-Liquid Displacement, Soc. Pet. Eng. J., pp. 17-25.

[12] Habermann, B. (1975): The Efficiency of Miscible Displacement as a Function of Mobility Ratio, SPE Reprint Series, No. 8, pp. 205-213.

[13] Warren, J.E. and Skiba, F.F. (1964): Macroscopic Dispersion, Soc. Pet. Eng. J. pp 215-230.

[14] Perrine, R.L. and Gay, G. M. (1966): Unstable Miscible Flow in Heterogeneous Systems, Soc. Pet. Eng. J. pp. 228-238.